PROJECT REPORT

On

NOVEL QUECERTIN SCHIFF BASES AS POTENT ANTI-INFLAMMATORY AGENTS

Submitted by

R. KRISHNANANDA (AB22CHE016)

In partial fulfilment for the award of the

Bachelor's Degree in Chemistry

DEPARTMENT OF CHEMISTRY AND CENTRE FOR RESEARCH

ST. TERESA'S COLLEGE (AUTONOMOUS)
ERNAKULAM

2024-2025

DEPARTMENT OF CHEMISTRY AND CENTRE FOR RESEARCH

ST. TERESA'S COLLEGE (AUTONOMOUS)

ERNAKULAM

B.Sc. CHEMISTRY PROJECT REPORT

Name	**: R. KRISHNANANDA**
Register Number	**: AB22CHE016**
Year of Work	**: 2024-2025**

This is to certify that the project **"NOVEL QUERCETIN SCHIFF BASES AS POTENT ANTI-INFLAMMATORY AGENTS"** is the work done by **R. KRISHNANANDA.**

Dr. Saritha Chandran.A.
Head of the Department

Dr. A. A. Shanty
Staff-member in charge

Submitted to the Examination of Bachelor's Degree in Chemistry

Date:.....

Examiners:.....

:.....

DEPARTMENT OF CHEMISTRY AND CENTRE FOR RESEARCH

ST. TERESA'S COLLEGE (AUTONOMOUS)

ERNAKULAM

CERTIFICATE

This is to certify that the project work entitled **"NOVEL QUERCETIN SCHIFF BASES AS POTENT ANTI-INFLAMMATORY AGENTS"** is the work done by **R. KRISHNANANDA** under my guidance in the partial fulfilment of the award of the Degree of Bachelor of Science in Chemistry at St. Teresa's College (Autonomous), Ernakulam affiliated to Mahatma Gandhi University, Kottayam.

Dr. A. A. SHANTY

Project Guide

DECLARATION

I hereby declare that the project work entitled **"NOVEL QUERCETIN SCHIFF BASES AS POTENT ANTI-INFLAMMATORY AGENTS"** submitted to Department of Chemistry and Centre for Research, St. Teresa's College (Autonomous) affiliated to Mahatma Gandhi University, Kottayam, is a record of an original work done by me under the guidance of **Dr. A. A. Shanty,** Assistant Professor, Department of Chemistry and Centre for Research, St. Teresa's College (Autonomous), Ernakulam and this project work is submitted in the partial fulfilment of the requirements for the award of the Degree of Bachelor of Science in Chemistry.

R. KRISHNANANDA

Acknowledgements

With deep appreciation, I wish to recognize the great almighty for his constant support, which serves as the most powerful instrument for the success and accomplishment of this project. I would like to convey my appreciation to my mentor, Dr. A.A. Shanty, Assistant Professor in the Department of Chemistry, St. Teresa's College, Ernakulam, who consistently inspired me. This project would not have been achievable without her guidance and encouragement.

I express my heartfelt gratitude to Rev. Sr. Nilima CSST, the Manager, Rev. Sr. Francis Ann CSST, the Director, Dr. Alphonsa Vijaya Joseph, the Principal, Dr. Saritha Chandran A., the Head of the Department of Chemistry, and all the faculty members of the Department of Chemistry at St. Teresa's College (Autonomous), Ernakulam for providing the necessary requirements for this project and consistent support. Furthermore, i would like to extend my thanks to all the non-teaching staff of the Department of Chemistry for their tremendous assistance throughout our project. I also appreciate and thank my parents and friends who have continuously supported and uplifted me morally.

R. KRISHNANANDA

Contents

Chapter 1

Introduction

1.1 QUERCETIN

Quercetin (2-(3,4-dihydroxyphenyl)-3,5,7-trihydroxy-4H-chromen-4-one) (*Figure1.1*) is a plant based flavanol belongs to flavonoid group of polyphenols, commonly found in fruits and vegetables like apple, strawberry, grape, red onion, lettuce, and broccoli. The identification and isolation of Quercetin was done by the Nobel Prize winner Szent-Gyorgyi [1]. Quercetin contains five hydroxyl group at 3,5,7,3' and 4' positions. Quercetin is widely known for its anti-oxidant, anti-inflammatory, anti-depressant, anti-diabetic, anticarcinogenic, anti-obesity and anti-malarial properties.

Quercetin has a molecular formula $C_{15}H_{10}O_7$ and a molecular mass of 302.236 g/mol. It is a yellow crystalline solid having bitter taste which is insoluble in water, partially soluble in alcohol and lipids and soluble in alkaline solutions [2]. The biosynthesis of flavonoids is a defense mechanism by plants in environment. Flavonoids protect internal tissues of plants from ultraviolet rays and prevent peroxidation of lipids[3].

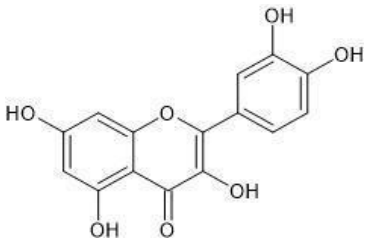

Figure 1.1: 2-(3,4-dihydroxyphenyl)-3,5,7-trihydroxy-4H-chromen-4-one

1.2 BIOLOGICAL PROPERTIES OF QUERCETIN

1.2.1 Antioxidant Property

The human body comprises an antioxidant defense system to protect cells from damages done by free radicals, ROS, and other reactive species. Antioxidant molecules scavenge free radicals from cells in our body and prevent damages from oxidation. Free radicals can oxidize macromolecules, such as DNA, proteins, carbohydrates, and lipids. Free radicals are compounds that can cause harm with increase in the level in our body, which include heart diseases and certain cancers. Reactive oxygen species (ROS) and reactive nitrogen species (RNS), also referred to as reactive species (RSs), react to produce all these health issues.

Quercetin could be beneficial against smoking which causes a formation of free radicals, ROS and toxic chemicals that is associated with increase in cardiovascular diseases. Cigarette tar is a source of free radicals which has been found to damage erythrocyte membranes. It has been found that quercetin and its derivatives could protect erythrocytes from the membranous damage caused by smoking[4]. Quercetin has been identified as a promising antioxidant that offers protection to hepatic HepG2 cells from oxidative stress linked to hyperglycemia[5]. Hyperglycemia is a condition of elevated blood glucose levels, a hallmark characteristic of diabetes mellitus, a group of metabolic diseases where the body either does not produce enough insulin or cannot effectively use the insulin it produces, leading to chronic hyperglycemia.

1.2.2 Antimicrobial Property

Over the decades, the incidence of infections has increased and microorganisms have become resistant to antibiotics, which eventually complicates medical treatment. The ineffectiveness of currently available antibiotic drugs has prompted the search for new types of antibacterial agents[5]. A wide range of polyphenols has proven to be potential anti-microbial agents. Quercetin is an antibacterial agent against wide range of bacterial strains mainly effecting gastrointestinal, respiratory, urinary, and integumentary systems. In general, Gram-negative bacteria are more resistant to anti-bacterial effects of Quercetin than Gram-positive bacteria, due to their impenetrable thick cell walls[6]. The antibacterial activity of quercetin and quercetin derivatives against different bacterial species occurred at different minimum inhibitory concentrations (MICs).

It has been observed quercetin's antibacterial effects on the growth of eleven main oral pathogenic microbes. Quercetin hindered the growth of six out of the eleven tested microbes including *Streptococcus mutans*, Streptococcussobrinus, *Lactobacillusacidophilu*, *Streptococcussanguis*, *Actinobacillus actinomycetemocomitans*, and *Prevotella intermedia* with MIC ranging from 1–8 mg/mL[7].

1.2.3 Anticancer Property

Quercetin has been considered as potential anticancer agent because it can inhibit cell proliferation and angiogenesis and induce apoptosis and cellular senescence. It can induce cell death and cell cycle arrest in cancer cells. The studies conducted with combination treatment of curcumin and quercetin on familial adenomatous polyposis (FAP) patients. The patients

were administered with 480 mg curcumin and 20 mg quercetin orally 3 times a day for 6 months. At the end of the study, curcumin and quercetin reduced the number and size of ileal and rectal adenomas with minimal adverse effects[8].

Recent research revealed that treatment of Michigan Cancer Foundation-7 (MCF-7) cancer cells (breast cancer cells) with quercetin enhances apoptosis and mRNA expression levels[9]. In the treatment of ovarian cancer, which is a fatal reproductive cancer, platinum drugs (i.e., cisplatin, oxaliplatin) are used usually. However, these drugs have side effects and lead to drug resistance. In a study with two human epithelial ovarian cancer cell lines (A2780 and its cisplatin resistant form $A2780^{cisR}$), the administration of Quercetin 2 h before the usage of platinum drugs might sensitize cancer cells to the action of platinum drugs and would be beneficial in dealing with the development of drug resistance[10].

1.2.4 Anti-Inflammatory Property

Anti-inflammatory is the property of a substance to reduce redness, swelling and pain in the body, and anti-inflammatory agents can block the substances which cause the inflammation. Quercetin possesses anti-inflammatory potential that can be expressed on both animal and human cells. It has been confirmed that quercetin anti-inflammatory effect is due to inhibition of proinflammatory cytokines, ATP, and nuclear factor kappa B (IkBa) binding sites[11]**.** Quercetin was proved to reduce pain and inflammation associated with arthritis[12].

Quercetin has shown anti-inflammatory properties in patients with coronary artery disease (CAD), by decreasing the transcriptional activity of the NF-kB. The study involving 85 CAD patients, stable angina pectoris, functional class II, and heart failure. Thirty patients received Quercetin at a daily dose of 120 mg for 2 months, while remaining 55 patients considered as the control group received β-blockers, statins, and aspirin. The influence of Quercetin has reduced the levels of IL-1β, IL-10 and TNF-α. Also, Quercetin decreased the expression of the inhibitor of kappa βα (Ikβα) gene relative to the control group[13].

1.3 SCHIFF BASE

Schiff Base, named after Hugo Joseph Schiff, have been known since middle of the nineteenth century. Schiff Base is a compound with the general structure $R_1R_2C=NR_3$ where R_3 is not equal to hydrogen. They can be considered as a sub class of imines. Imine is a functional group or chemical compound containing a carbon-nitrogen double bond. The nitrogen atom can be attached to hydrogen or an organic compound (R). If this group is not a hydrogen atom, then the compound can be sometimes referred as a Schiff base. Schiff Base Reaction is a condensation reaction in which primary amine reacts with ketones or aldehyde to form Schiff Base as major product and water as minor product where R, may be alkyl or an aryl group (*Figure 1.2*).

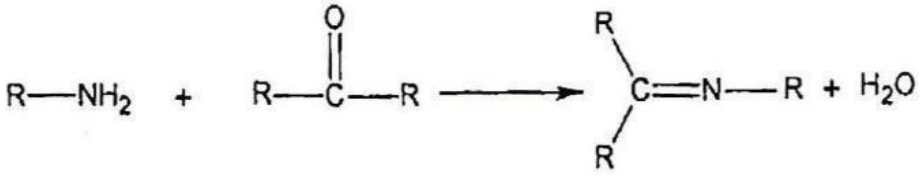

Figure 1.2: Condensation reaction of amines with ketone or aldehyde to form Schiff base

Schiff Base that contains aryl substituent are substantially more stable and more readily synthesized, while those which contains alkyl substituents are relatively unstable. Schiff base of aliphatic aldehydes is relatively unstable and readily more polymerizable while those of aromatic aldehydes having effective conjugation are more stable.

1.3.1 Application of Schiff Base compound

Schiff bases have gained significant attention in medicinal and pharmaceutical fields due to their broad spectrum of biological activities. The azomethine nitrogen atom can participate in hydrogen bonding with active centers of cellular components, disrupting normal cellular processes. Chiral Schiff bases were among the first ligands employed in asymmetric catalysis. In 1968, Ryoji Noyori introduced a copper-Schiff base complex for the metal-carbenoid cyclopropanetrione of styrene. His contributions earned him a share of the 2001 Nobel Prize in Chemistry. Chromium azomethine complexes, cobalt Schiff base complexes, and unsymmetrical 1:2 complexes are widely used for imparting fast colours to materials such as leather, food packaging, and wool. Schiff bases are known for their excellent light resistance, durability, and stability even in the presence of acidic gases like CO_2. Additionally, novel tetradentate Schiff bases serve as chromogenic reagents for detecting nickel in natural food samples. For instance, Schiff bases are used as fabric dyes, providing different colours when combined with various mordants. In agriculture, Schiff bases exhibit several beneficial properties, including: insecticidal activity, antifungal properties, nutrification inhibition and role in Coordination Chemistry. Schiff bases are common ligands in coordination chemistry due to the basic nature of the imine nitrogen and its π-acceptor

capabilities. These ligands are typically synthesized from alkyl diamines and aromatic aldehydes.

1.3.2 Biological Activities of Schiff Bases

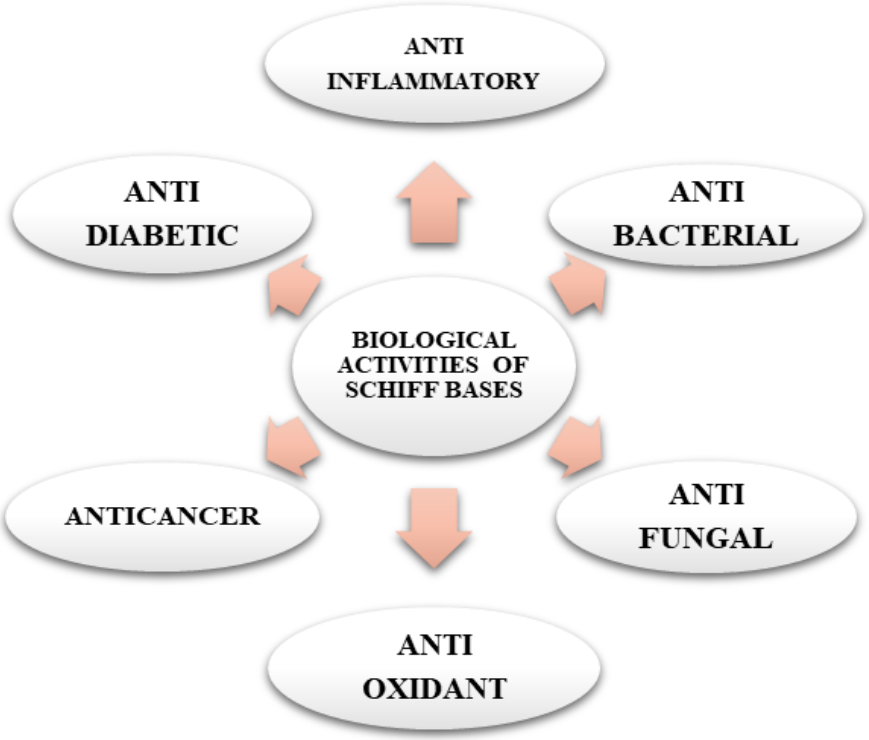

Figure 1.3: Biological applications of Schiff bases

1.4 INFLAMMATION

Inflammation is a local protective response of living tissues due to any injury, infection or harmful stimuli[14]. It is derived from the Latin word '*inflammatio*' which means to "set on fire" as it is a body's response in the form of heat, pain, swelling, redness, etc. when inflammation occurs, the

body release inflammatory mediators which includes hormones like bradykinin and histamine. These increases the blood flow towards the affected area which in turn appears to be warm and red in color[15].

1.4.1 Steps involving inflammation

1. When an injury occurs in a particular body part, chemical signals such as histamine are released which activates specialized white blood cells or macrophages to the injured region and capillaries across the region will become wider and more permeable (*Figure 1.4*)
2. Blood flow increases across the region and initiates clotting process
3. Phagocytes engulfs the death cells, bacteria or any foreign substances present around the region i.e., phagocytosis takes place and the wound starts to heal.

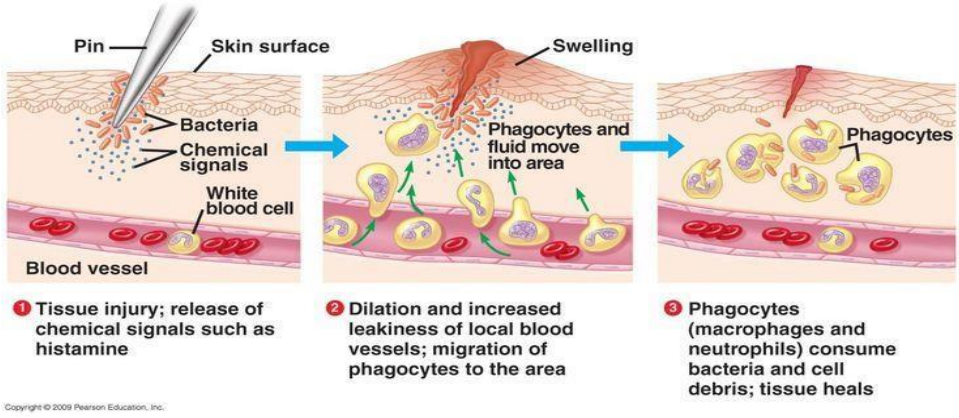

Figure 1.4: steps involving inflammation

1.4.2 Types of inflammation

1. Acute inflammation: acute inflammation is short time protective response when the body sustain to any infection, injuries or when a

foreign body attacks the immune system[16].

2. Chronic inflammation: it is a serious long-term inflammation which can prolong up to several months or years. It can happen due to many different reasons such as failure of eliminating the foreign body which is responsible for inflammation, autoimmune diseases, or even repeated episodes of acute inflammation[17].

1.4.3 Causes of Inflammation

Inflammation, the body's defense mechanism against damage, arises from a variety of triggers. Pathogens like bacteria, viruses, and fungi initiate an immune response, targeting these invaders within the body. Physical injuries, such as cuts and wounds, and the presence of foreign objects also induce inflammation to facilitate healing. Irritants and toxins, including chemicals, pollutants, and radiation, can damage tissues and trigger an inflammatory reaction. Additionally, autoimmune disorders mistakenly activate the immune system to attack healthy tissues, resulting in chronic inflammation, as seen in conditions like rheumatoid arthritis and lupus. Lifestyle factors significantly contribute to inflammatory processes; processed foods, obesity, chronic stress, lack of exercise, smoking, and poor sleep can all promote chronic inflammation. While acute inflammation is a short-term, beneficial response to injury or infection, chronic inflammation poses risks to various long-term health problems (*Figure 1.5*).

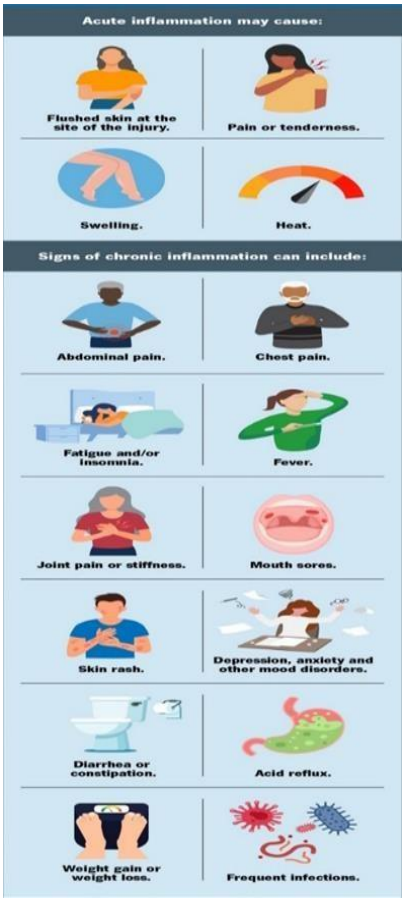

Figure 1.5: Symptoms of inflammation

1.4.4 Prevention of Inflammation

Research indicates that adopting an anti-inflammatory diet can significantly mitigate inflammation. The Mediterranean diet, rich in foods with anti-inflammatory properties such as fatty fish, vibrant fruits and vegetables, whole grains, and healthy fats is a prime example. Furthermore, the National Institutes of Health recognizes weight loss as a highly effective strategy for reducing chronic inflammation. To achieve this, it is advisable to increase the intake of fruits, vegetables, and whole grains, and to engage in at least 150 minutes of moderate-intensity

physical activity each week. Beneficial activities include aerobic exercise, weight training, and resistance training. Additionally, relaxation practices such as meditation, yoga, biofeedback, guided imagery, or deep breathing can promote stress reduction, even in short sessions.

Prioritizing sleep is essential; aim for 7 to 9 hours per night, maintaining a consistent sleep schedule, turning off screens before bedtime, and ensuring a dark, cool sleeping environment. It is also important to avoid smoking and tobacco products, maintain a healthy weight, and limit alcohol consumption. Consult with a healthcare professional regarding strategies to minimize exposure to harmful pollutants or toxic substances. Short-term stress can be a motivator and protective mechanism, but chronic stress significantly elevates inflammation through the release of hormones like cortisol. Therefore, implementing a stress management routine—including mindfulness, deep breathing, exercise, or yoga is crucial. Effective stress management also alleviates chronic pain, as the two are closely linked, and facilitates the release of chemicals that aid in healing injuries, combating infections, and clearing cellular debris.

1.4.5 Anti-Inflammatory Drugs

Anti -inflammatory drugs combat inflammation, reduce pain and related symptoms under various conditions. These drugs come in many categories, in which nonsteroidal anti-inflammatory drugs (NSAIDs) are widely accessible by over-the-counter and prescription. NSAIDS functions by preventing prostaglandin production, thus reduces pain and inflammation. Common examples include ibuprofen, naproxen, and aspirin. For more severe inflammatory conditions, corticosteroids,

powerful anti-inflammatory drugs, which mimic cortisol, are determined, administered orally, or administered by the injection. Additionally, other specific anti-inflammatory drugs exist to target specific inflammatory routes, often used in autoimmune diseases. Effective, anti-inflammatory drugs can cause side effects (*Table 1*). NSAIDs can worsen the stomach and increase the risk of bleeding, and corticosteroids, especially with prolonged use, can cause more important adverse effects. Therefore, it is important to consult a healthcare professional before starting any anti - inflammatory drug, especially for persons with already existing health issues.

ANTI INFLAMMATORY DRUGS	**DISEASES TREATED**	**SIDE EFFECTS OF THE DRUG**
Aspirin (Acetylsalicylic acid)	Lower the risk of heart attack, stroke and used as anti-clotting agent	Can have severe headache, asthma attack, tinnitus etc.
Naproxen or (S)- 2-(6-Methoxy-naphthalen-2-yl)-propionic acid	Osteoarthritis, rheumatoid arthritis, or juvenile arthritis	Indigestion, heartburn, stomach pain, nausea
Ibuprofen (RS)-2-(4-(2-methylpropyl) phenyl) propanoic acid	Rheumatoid disorders, mild to moderate pain, fever, dysmenorrhea, and osteoarthritis	Nausea, indigestion, dizziness, headache
Diclofenac or 2-[2-(2,6-dichloroanilino) phenyl] acetic acid	Osteoarthritis or rheumatoid arthritis	Constipation, diarrhea, loss of appetite, dizziness
Meloxicam	Juvenile rheumatoid arthritis, osteoarthritis, and rheumatoid arthritis	Bleeding gums, blood in urine, stomach pain, canker soars

Table 1: Anti-inflammatory drugs, treatment, side effects

Chapter 2

Materials and Methods

2.1 MATERIALS

2.1.1 Reagents

1) Quercetin
2) 4-Aminoantipyrine
3) 3-Aminobenzoic acid
4) 2-Amino-5-methylpyridine
5) Sulfanilamide

2.1.2 Solvents

1) Methanol
2) Ethanol
3) Petroleum ether
4) DMSO

2.2 EXPERIMENTAL METHODS

2.2.1 Elemental Analysis

Elemental analysis is a process to analyze the elemental composition of a sample. The analysis can be qualitative and quantitative. It can be performed on wide range of sample types including solids, liquids, and volatile substances. CHN elemental analyzers commonly utilize high temperature combustion analysis in an environment rich in oxygen. Upon combustion, the elements present are converted into simultaneous oxide

gas states and detection of these gases can be carried out via different methods.

Carbon, hydrogen, and nitrogen content in all the synthesized compounds were analyzed by using a Vario EL CHNS analyzer at Sophisticated Test Instrumentation Centre (SAIF), Cochin University of Science and Technology, Kochi, India.

2.2.2 UV-Visible Spectroscopy

Electronic or Ultraviolet-visible Spectroscopy is an analytical technique used for characterizing different types of organic, inorganic, and biological materials. It deals with UV-visible region (100-800 nm) of electronic spectrum by measuring the number of wavelengths of UV and visible light that are absorbed or transmitted through a sample comparing with a reference sample. The absorption of electromagnetic radiation in UV-vis region by a molecule or atom or ion gives electronic transitions in various energy levels. The possible transitions are $\pi \rightarrow \pi^*$, $n \rightarrow \pi^*$, $\sigma \rightarrow \sigma^*$, and $n \rightarrow \sigma^*$. UV-visible spectrum is plotted as absorbance against wavelength in nm.

UV-visible spectra of the synthesized samples were recorded in methanol on a Thermo electron Nicolet Evolution 300 UV-vis Spectrometer.

2.2.3 FT-IR Spectroscopy

Infrared spectroscopy is a molecular spectroscopic technique in which atoms or molecules absorb infrared radiation to undergo vibrational transitions. The IR spectrum gives information about the nature of functional groups such as carbonyl group, hydroxyl group in solid, liquid, or gaseous state. The Fourier Transform Infrared is the preferred method of IR spectroscopy. The IR spectrum can be divided into three main

regions: the far-IR (<400 cm-1), the mid-IR (4000-400 cm-1), and the near-IR (13000-4000 cm-1). Many applications employed in the mis-IR region. The mid-IR region can be further divided into; X-H stretching region (4000-2500 cm-1), the triple-bond region (2500-200 cm-1), double-bond region (2000-1500 cm-1), and finger-print region (1500-600 cm-1). Infrared spectra of the samples were recorded on a JASCO FT-IR 5300 Spectrometer in the range 4000-400 cm^{-1} using KBr pellets at the Central Instrumentation Facility at Bharata Mata College.

2.2.4 Nuclear Magnetic Resonance Spectroscopy

The NMR spectroscopy is a technique used to study molecules by recording the transition between spin energy levels of nuclei present in sample in an applied magnetic field by absorption of radio waves. NMR spectrum is a plot of the intensity of absorption against frequency. Spectrum typically appears in 10-800 MHz frequency and positions of lines in ppm using chemical shift scale. The absorption position of a particular proton from the absorption position of a reference proton is called the chemical shift of the proton. From identifying the purity and composition of sample to study the magnetic properties of various nuclei, it gives a clear idea of the different properties possessed by the sample. ^{1}H NMR spectroscopy provides insight into the hydrogen atoms and their interactions, and ^{13}C NMR spectroscopy provides structural information about the carbon atoms in a molecule.

The ^{1}H and ^{13}C NMR spectra detected using $CDCl_3$ on a Bruker Advance DRX 300NFT- NMR Spectrometer at SAIF, CUSAT with TMS as the standard.

2.2.5 Fluorescence Spectroscopy

Fluorescence spectroscopy is an instrumental technique that utilizes a specialized instrument (Spectrofluorophotometer) to measure and study the radiations emitted by the sample. It measures the intensity of the emitted fluorescence at specific wavelength, allowing the identification and quantification of fluorescence of fluorescent molecules of the sample. It has a wide range of applications in areas of research like pharmaceuticals, chemical, life science, food science, environmental monitoring and even used to study biological phenomenon like bioluminescence and chemical phenomenon like chemiluminescence. Some other applications include research and development of fluorescent dyes and protein analysis.

Fluorescence spectra of the synthesized Schiff bases were recorded in methanol using Spectrofluorophotometer RT-6000 at Teresian Instrumental and Consultancy Centre (TICC).

2.2.6 Anti-Inflammatory Study

The anti-inflammatory tests were done using HRBC stabilization method.

Materials

- Human blood
- Alsever solution
- Isosaline
- Synthesized Schiff bases

Procedure

Fresh whole human blood was collected. It was mixed with an equal volume of sterilized Alsever solution containing 2% dextrose, 0.8%

sodium citrate, 0.05% citric acid, 0.42% sodium chloride in water. The blood mixture was centrifuged at 3000 rpm for 10 minutes. Packed cells were washed three times with isosaline (0.85%, pH 7.2). The blood volume was measured and reconstituted as a 10% v/v suspension with isosaline. For the Anti-inflammatory Assay, 1mL of the prepared HRBC suspension was mixed with an equal volume of plant extracts at five concentrations: 0.5 mg/mL, 2.5 mg/mL, 5 mg/mL, 10 mg/mL, and 12.5 mg/mL. Diclofenac sodium (50 mg/mL) was used as a standard. The assay mixtures (HRBC suspension + plant extract) were incubated at 56°C for 30 minutes to stabilize the HRBC membranes. Post-incubation, the mixtures were centrifuged at 3000 rpm to separate intact RBCs from the supernatant. The absorbance of the supernatant was measured at 560 nm using a spectrophotometer to quantify haemoglobin.

Percentage of protection = 100-OD of test/OD of control * 100
Control of OD = 1.179

2.3 SYNTHESIS OF SCHIFF BASE

2.3.1 Synthesis of Schiff base from Quercetin and 4-amino antipyrine (QAAP)

Quercetin and 4-aminoantipyrene in methanol were combined in 1:1 ratio and heated for 6 hours under reflux in a round-bottom flask (*Scheme1*). After cooling and being concentrated, the obtained solution is allowed to undergo slow evaporation. The precipitate collected after filtering, and washing with ethanol is recrystallized and dried. Crystals with a brown hue were obtained (*Figure 2.1*).

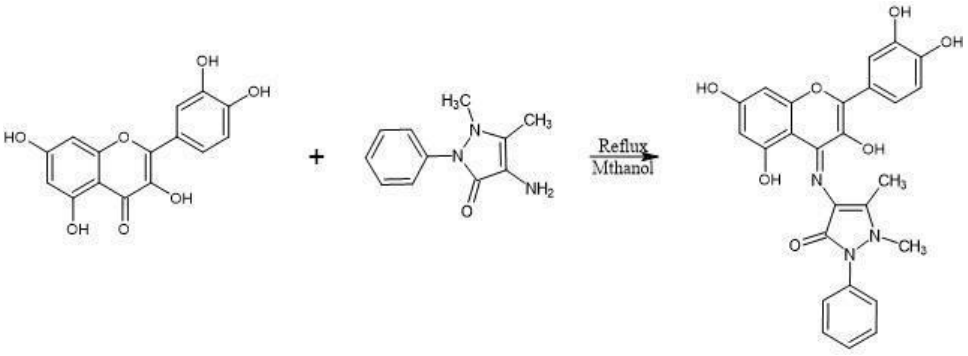

Scheme 1: Preparation of Schiff base QAAP

Figure 2.1: Crystals of QAAP

2.3.2 Synthesis of Schiff base from Quercetin and 3-aminobenzoic acid (QABD)

Quercetin and 3-aminobenzoic acid in methanol were combined in 1:1 ratio and heated for 6 hours under reflux in a round-bottom flask (*Scheme2*). After cooling and being concentrated, the obtained solution is allowed to undergo slow evaporation. The precipitate collected after filtering, and washing with ethanol is recrystallized and dried. Crystals with a yellow hue were obtained (*Figure 2.2*).

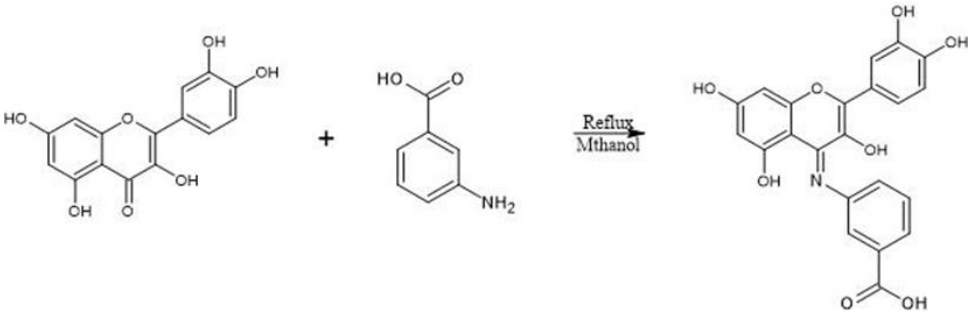

Scheme 2: Preparation of Schiff base QABD

Figure 2.2: Crystals of QABD

2.3.3 Synthesis of Schiff base from Quercetin and 2-amino-5-methylpyridine (QAMP)

Quercetin and 2-amino-5-methylpyridine in methanol were combined in 1:1 ratio and heated for 6 hours under reflux in a round-bottom flask (*Scheme3*). After cooling and being concentrated, the obtained solution is allowed to undergo slow evaporation. The precipitate collected after filtering, and washing with ethanol is recrystallized and dried. Crystals with a yellow hue were obtained (*Figure 2.3*).

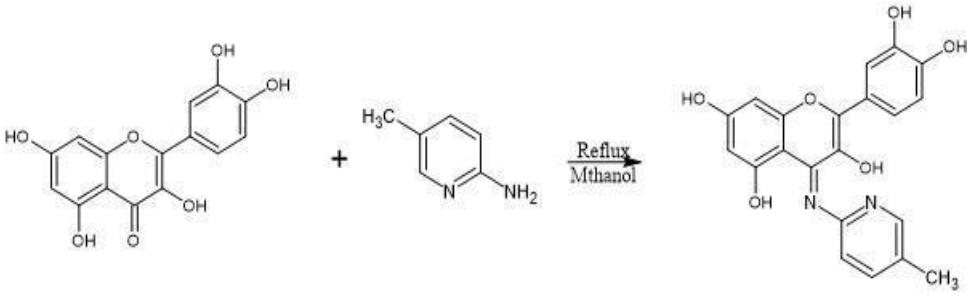

Scheme 3: Preparation of Schiff base QAMP

Figure 2.3: Crystals of QAMP

2.3.4 Synthesis of Schiff base from Quercetin and Sulfanilamide (QSAM)

Quercetin and sulfanilamide in methanol were combined in 1:1 ratio and heated for 6 hours under reflux in a round-bottom flask (*Scheme4*). After cooling and being concentrated, the obtained solution is allowed to undergo slow evaporation. The precipitate collected after filtering, and washing with ethanol is recrystallized and dried. Crystals with a green hue were obtained (*Figure 2.4*).

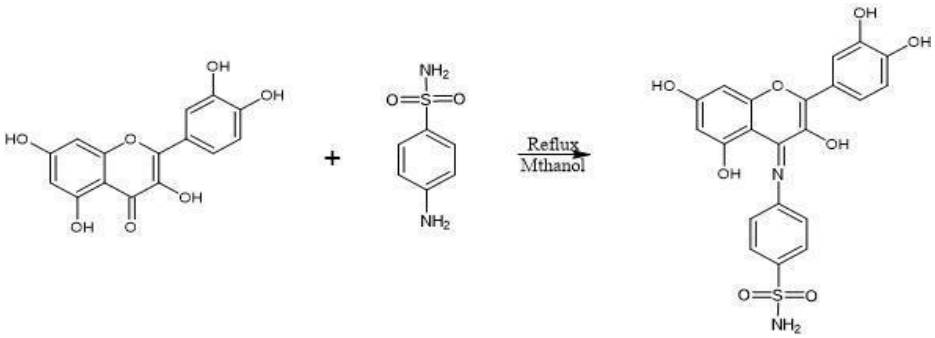

Scheme 4: Preparation of Schiff base QSAM

Figure 2.4: Crystals of QSAM

Chapter 3

Results and discussion

3.1 ANALYSIS OF QAAP (Quercetin+4-Aminoantipyrine)

3.1.1 Elemental Analysis

Elemental analysis of QAAP was conducted to examine the elemental composition of the Schiff base. QAAP has an empirical formula $C_{26}H_{21}O_7N_3$. The results obtained are consistent with the proposed chemical formula of the assigned structure (*Table 1)*.

Compound	Empirical Formula	Formula Weight	Colour	Found (Calculated %)		
				C	H	N
QAAP	$C_{26}H_{21}O_7N_3$	487.469	Brown	63.16 (65.09)	4.01 (4.09)	8.08 (8.23)

Table 1: Elemental analysis of QAAP

3.1.2 UV-Visible Spectroscopy

The chemical structure and optical characteristics of the sample QAAP were investigated using Ultraviolet-visible spectroscopy. The UV-visible spectrum of QAAP was obtained in methanol (*Figure 3.1*). In the UV-visible spectrum, the primary transitions are $\pi \rightarrow \pi^*$ for aromatic rings around 180-350 nm and $n \rightarrow \pi^*$ for azomethine groups (C=N) around 300-450 nm. The sample QAAP exhibit peaks at 261 nm for transition within aromatic rings and 375 nm for transition within C=N group.

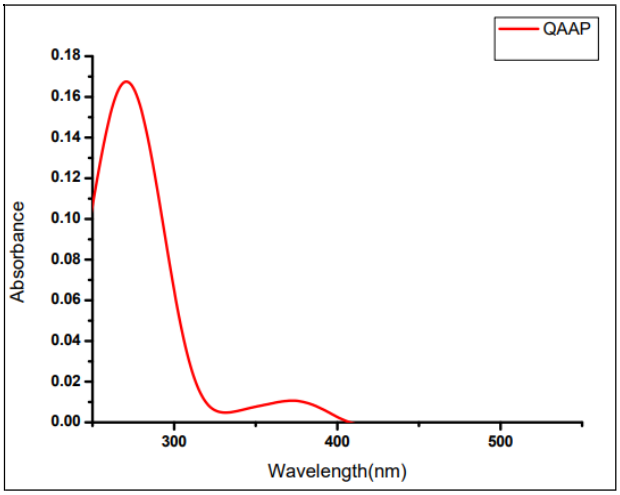

Figure 3.1: UV-visible spectrum of QAAP

3.1.3 Infrared Spectroscopy

The functional groups present and molecular structure of the sample QAAP were obtained from IR spectrum (*Figure 3.2*). A sharp peak at 1662.52 cm^{-1} was obtained for QAAP corresponding to the IR absorption peak of imine group (C=N) in the range 1600-1680 cm^{-1}. A peak at 3405.13 cm^{-1} was obtained corresponding to the absorption peak of phenolic (OH) group in the range 3500-3200 cm^{-1}.

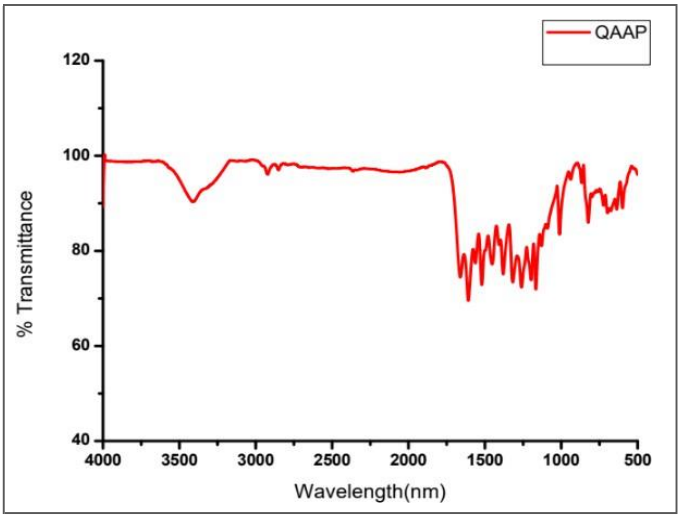

Figure 3.2: IR spectrum of QAAP

3.1.4 Nuclear Magnetic Resonance Spectroscopy

3.1.4.1 ^{1}H NMR Spectroscopy

^{1}H NMR spectrum of the sample QAAP (*Figure 3.3*) provides the information about the number of hydrogen atoms and their relationships.

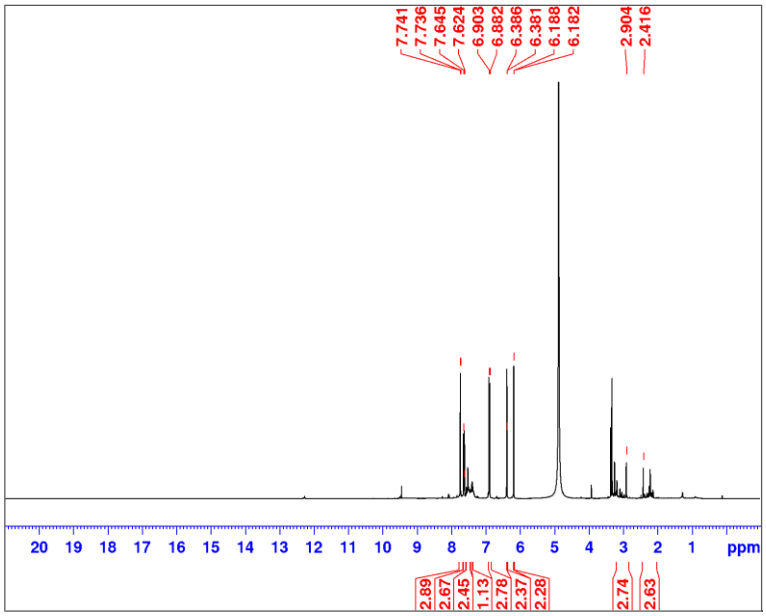

Figure 3.3: ^{1}H NMR spectrum of QAAP

^{1}H NMR (CH_3OH δ ppm): 2.4 (3H, C-H), 2.9 (3H, C-H), 6.1 (2H, Ar-H), 6.2 (1H, Ar-H), 6.3 (3H, Ar-H), 6.8 (2H, Ar-H), 6.9 (1H, Ar-H), 7.4 (1H, OH), 7.6 (2H, OH), 7.7 (1H, OH), 7.8 (1H, OH).

3.1.4.2 ^{13}C NMR Spectroscopy

^{13}C NMR spectrum of the sample QAAP (*Figure 3.4)* reveal the carbon skeleton of the compound.

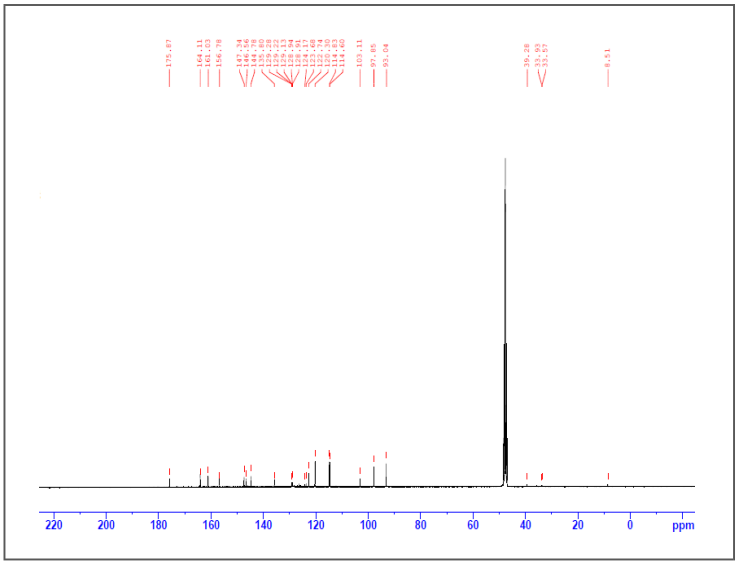

Figure 3.4: ^{13}C NMR spectrum of QAAP

^{13}C NMR (CH_3OH δ ppm): 33.57 (C-H), 39.28 (C-H), 93.04 (Ar-C), 97.85(Ar-C), 103.11(Ar-C), 114.60(Ar-C), 120.30(Ar-C), 122.74(Ar-C), 123.68, 124.27(Ar-C), 128.91, 129.13(Ar-C), 135.80 (Ar-OH), 144.78(Ar-OH), 146.56(Ar-C-OH),156.78(Ar-CO), 161.03(Ar-C-OH),164.11(Ar-C-OH), 175.87(ArC=N).

3.4.5 Fluorescence Spectroscopy

The photoluminescence properties of the sample QAAP was obtained from the fluorescence spectrum (*Figure 3.5*). QAAP was excited at 350 nm and an emission wavelength was obtained at 429 nm. The solid-state and liquid-state fluorescence were observed under UV light (*Figure 3.6, 3.7*). The liquid-state fluorescence was examined in methanol, acetone, hexane, ethyl alcohol and DMF.

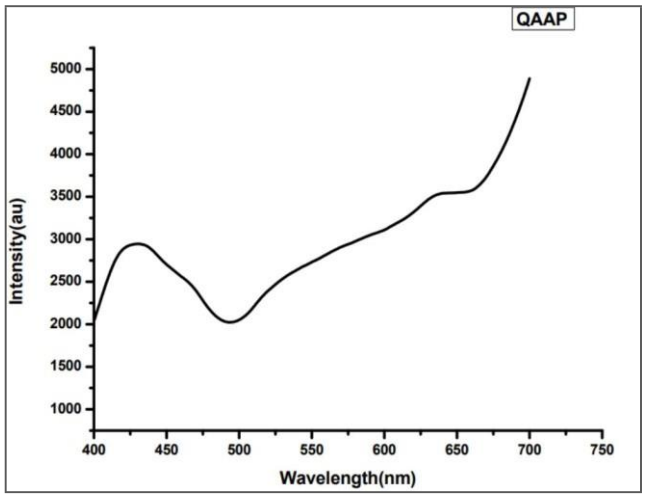

Figure 3.5: Fluorescence spectrum of QAAP

Figure 3.6: Solid-state fluorescence of QAAP

Green-yellow Orange Green-yellow

Figure 3.7: Liquid fluorescence of QAAP in methanol, acetone, hexane, ethyl alcohol and DMF

3.2 ANALYSIS OF QABD (Quercetin+3-Aminobenzoic acid)

3.2.1 Elemental Analysis

Elemental analysis of QABD was conducted to examine the elemental composition of the Schiff base. QABD has an empirical formula

$C_{22}H_{15}O_8N$.The results obtained are consistent with the proposed chemical formula of the assigned structure (*Table 2*).

Compound	**Empirical Formula**	**Formula Weight**	**Colour**	**Found (Calculated %)**		
				C	**H**	**N**
QABD	$C_{22}H_{15}O_8N$	421.366	Yellow	63.45 (65.72)	3.94 (4.11)	3.22 (3.46)

Table 2: Elemental analysis of QABD

3.2.2 UV-Visible Spectroscopy

The chemical structure and optical characteristics of the sample QABD were investigated using Ultraviolet-visible spectroscopy. The UV-visible spectrum of QABD was obtained in methanol (*Figure 3.8*). In the UV-visible spectrum, the primary transitions are $\pi \rightarrow \pi^*$ for aromatic rings around 180-350 nm and $n \rightarrow \pi^*$ for azomethine groups (C=N) around 300-450 nm. The sample QABD exhibit peaks at 260 nm for transition within aromatic rings and 370 nm for transition within C=N group.

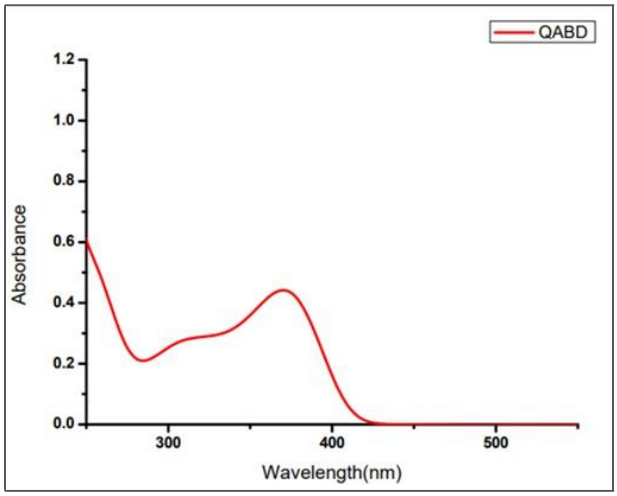

Figure 3.8: UV-visible spectrum of QABD

3.2.3 Infrared Spectroscopy

The functional groups present and molecular structure of the sample QABD were obtained from IR spectrum (*Figure 3.9*). A sharp peak at 1653.90 cm^{-1} was obtained for QABD corresponding to the IR absorption peak of imine group (C=N) in the range 1690-1640 cm^{-1}. A peak at 3405.71 cm^{-1} was obtained corresponding to the absorption peak of phenolic (OH) group in the range 3500-3200 cm^{-1}.

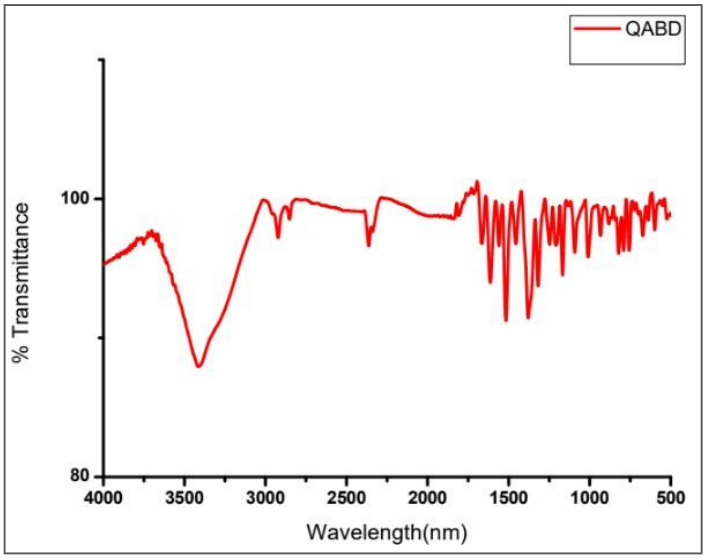

Figure 3.9: IR spectrum of QABD

3.2.4 Nuclear Magnetic Resonance Spectroscopy

3.2.4.1 ^{1}H NMR Spectroscopy

^{1}H NMR spectrum of QABD (*Figure 3.10*) provides the information about the number of hydrogen atoms and their relationships.

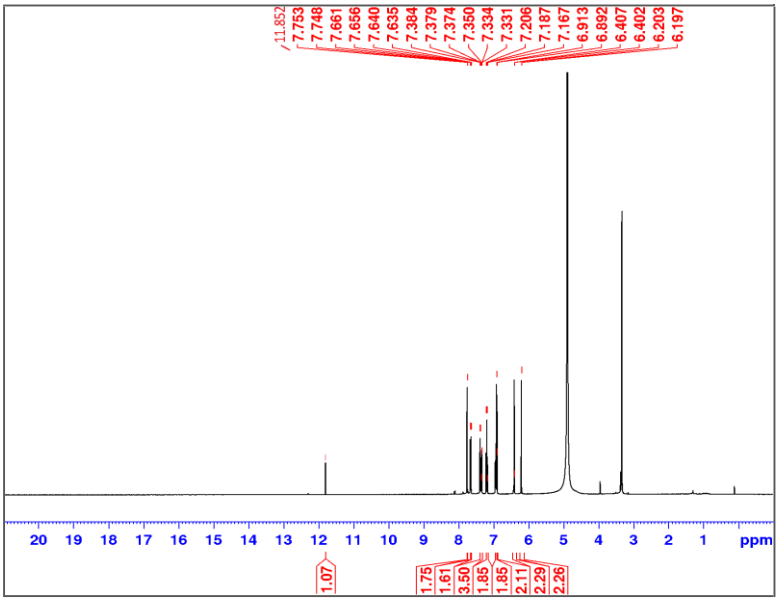

Figure 3.10: [1]H NMR spectrum of QABD

[1]H NMR (CH_3OH δ ppm): 6.2(2H, Ar-H), 6.9(2H, Ar-H), 6.8(2H, Ar-H), 6.9(1H, Ar-H), 7.1(1H, Ar-H), 7.2(2H, OH), 7.3(1H, OH), 7.6(2H, OH), 7.7(1H, OH), 11.8(1H, CH_3COOH)

3.2.4.2 [13]C NMR Spectroscopy

[13]C NMR spectrum of the sample QABD (*Figure 3.11)* reveal the carbon skeleton of the compound.

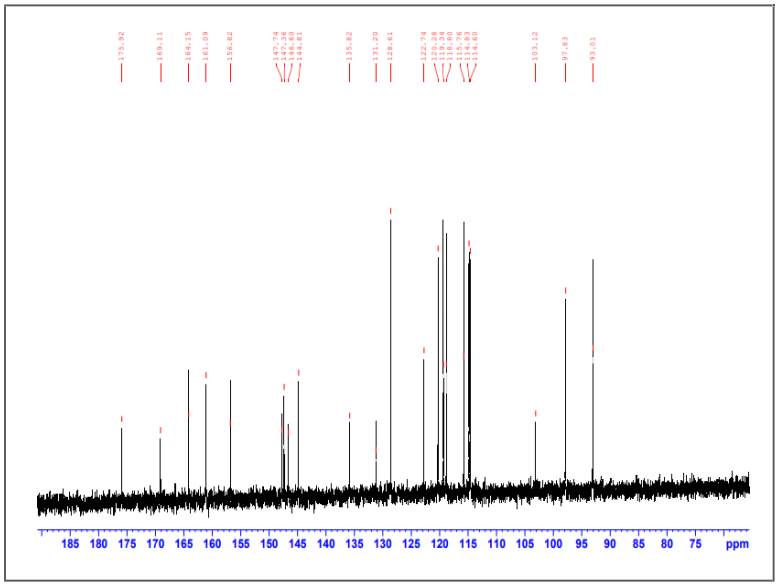

Figure 3.11: ^{13}C NMR spectrum of QABD

^{13}C NMR (CH_3OH δ ppm): 93.70 (Ar-C), 98.63 (Ar-C), 104.23(Ar-C), 114.29, 116.79(Ar-C), 120.031(Ar-C), 122.49(Ar-C), 130.28(Ar-C), 132.46(Ar-H), 136.24(Ar-H), 147.22(Ar-C-OH), 148.23(Ar-C-OH), 157.65(Ar-CO), 161.27(Ar-C-OH), 168.15(Ar-C-OH), 169.11(Ar-C-OH), 175.92(Ar-C=N).

3.4.5 Fluorescence Spectroscopy

The photoluminescence properties of the sample QABD was obtained from the fluorescence spectrum (*Figure 3.12*). QABD was excited at 350 nm and an emission wavelength was obtained at 430 nm. The solid-state and liquid-state fluorescence were observed under UV light (*Figure 3.13, 3.14*). The liquid-state fluorescence was examined in methanol, acetone, hexane, ethyl alcohol and DMF.

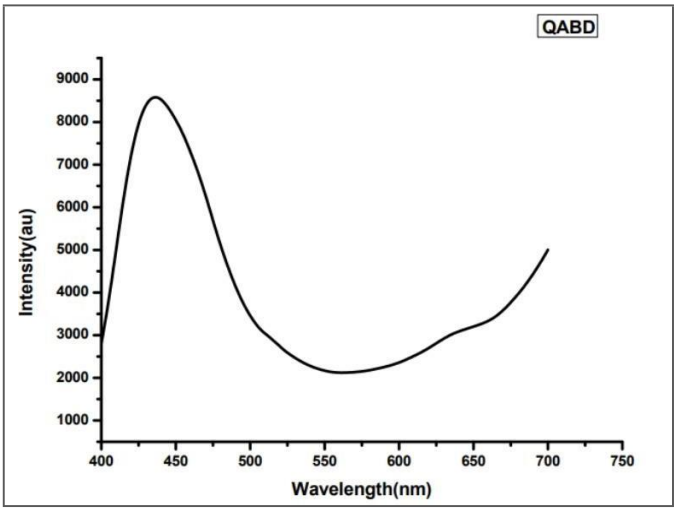

Figure 3.12: Fluorescence spectrum of QABD

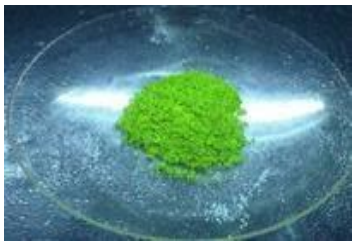

Figure 3.13: Solid-state fluorescence of QABD

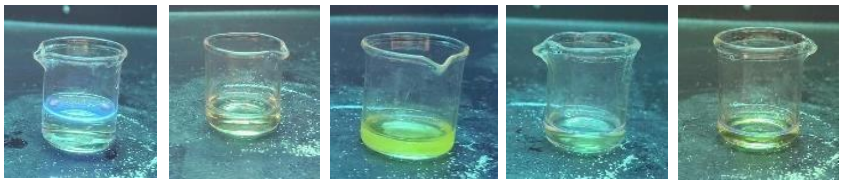

Blue Green-yellow

Figure 3.14: Liquid fluorescence of QABD in methanol, acetone, hexane, ethyl alcohol and DMF

3.3 ANALYSIS OF QAMP (Quercetin+2-Amino-5-methylpyridine)

3.3.1 Elemental Analysis

Elemental analysis of QAMP was conducted to examine the elemental composition of the Schiff base. QAMP has an empirical formula

$C_{21}H_{16}O_6N_2$.The results obtained are consistent with the proposed chemical formula of the assigned structure (*Table 3)*.

Compound	**Empirical Formula**	**Formula Weight**	**Colour**	**Found (Calculated %)**		
				C	**H**	**N**
QAMP	$C_{21}H_{16}O_6N_2$	392.369	Yellow	64.45 (64.98)	3.86 (3.97)	7.16 (7.25)

Table 3: Elemental analysis of QAMP

3.3.2 UV-Visible Spectroscopy

The chemical structure and optical characteristics of the sample QAMP were investigated using Ultraviolet-visible spectroscopy. The UV-visible spectrum of QAMP was obtained in methanol (*Figure 3.15*). In the UV-visible spectrum, the primary transitions are $\pi \rightarrow \pi^*$ for aromatic rings around 180-350 nm and $n \rightarrow \pi^*$ for azomethine groups (C=N) around 300-450 nm. The sample QAMP exhibit peaks at 260 nm for transition within aromatic rings and 377 nm for transition within C=N group.

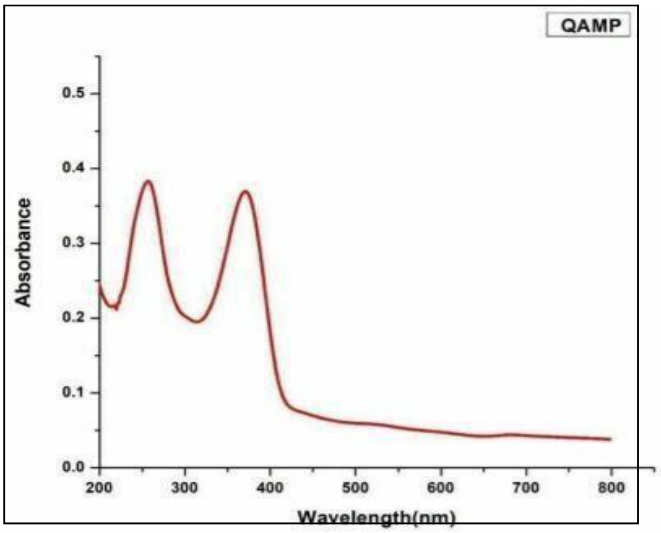

Figure 3.15: UV-visible spectrum of QAMP

3.3.3 Infrared Spectroscopy

The functional groups present and molecular structure of the sample QAMP were obtained from IR spectrum (*Figure 3.2*). A sharp peak at 1662.10 cm^{-1} was obtained for QAMP corresponding to the IR absorption peak of imine group (C=N) in the range 1690-1640 cm^{-1}. A peak at 3405.67 cm^{-1} was obtained corresponding to the absorption peak of phenolic (OH) group in the range 3500-3200 cm^{-1}.

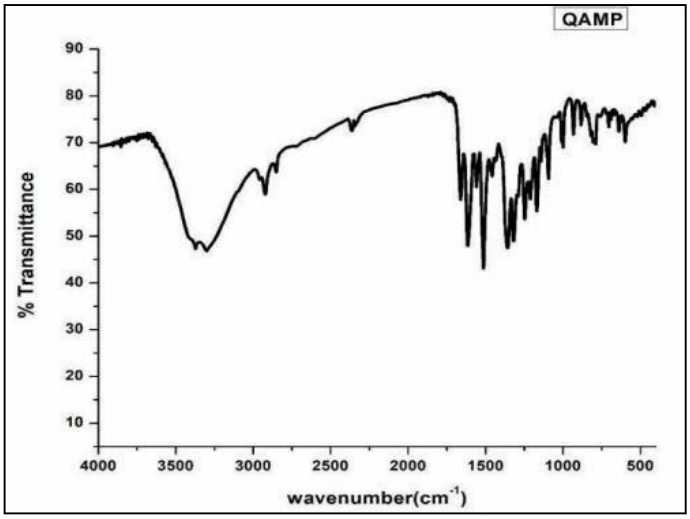

Figure 3.16: IR spectrum of QAMP

3.3.4 Nuclear Magnetic Resonance Spectroscopy

3.3.4.1 ^{1}H NMR Spectroscopy

^{1}H NMR spectrum of QAMP (*Figure 3.17*) provides the information about the number of hydrogen atoms and their relationships.

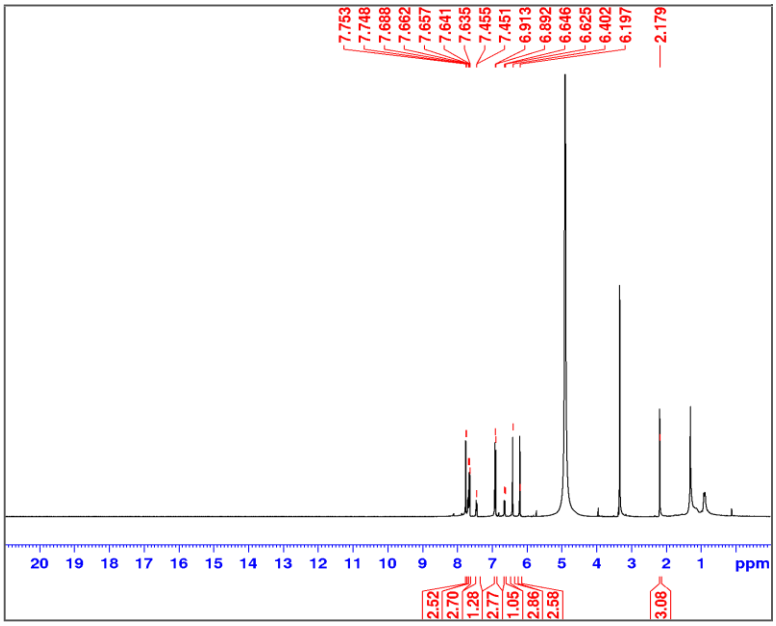

Figure 3.17: [1]H NMR spectrum of QAMP

[1]H NMR (CH_3OH δ ppm): 2.1(3H, C-H), 6.2(1H, Ar-H), 6.4(2H, Ar-H), 6.6(1H, Ar-H), 6.8(2H, Ar-H), 6.9(1H, Ar-H), 7.2(1H, Ar-H), 7.4(1H, OH), 7.6(2H, OH), 7.7(1H, OH), 7.8(2H, OH).

3.3.4.2 ^{13}C NMR Spectroscopy

^{13}C NMR spectrum of the sample QAMP (*Figure 3.18)* reveal the carbon skeleton of the compound.

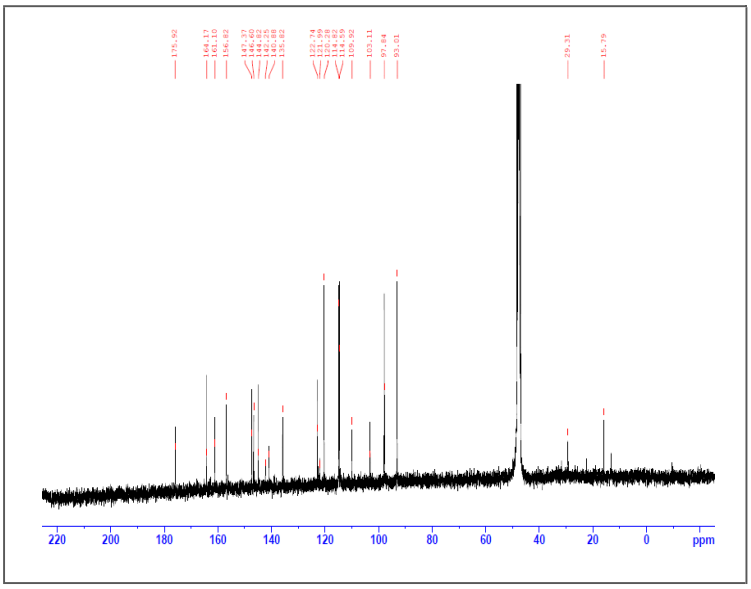

Figure 3.18: ^{13}C NMR spectrum of QAMP

^{13}C NMR (CH_3OH δ ppm): 29.31(C-H), 93.01(Ar-C), 97.84(Ar-C), 103.12(Ar-C), 109.92(Ar-C), 114.59, 114.82(Ar-C), 120.28(Ar-C), 121.99(Ar-C), 122.74(Ar-C), 135.82(Ar-OH), 140.88(Ar-OH), 144.81(Ar-C), 146.60(Ar-C-OH), 147.37(Ar-CO), 156.82 (Ar-CO),161.10(Ar-C-OH),175.92(ArC=N).

3.4.5 Fluorescence Spectroscopy

The photoluminescence properties of the sample QAMP was obtained from the fluorescence spectrum (*Figure 3.19*). QAMP was excited at 350 nm and an emission wavelength was obtained at 429 nm. The solid-state and liquid-state fluorescence were observed under UV light (*Figure 3.20, 3.21*). The liquid-state fluorescence was examined in methanol, acetone, hexane, ethyl alcohol and DMF.

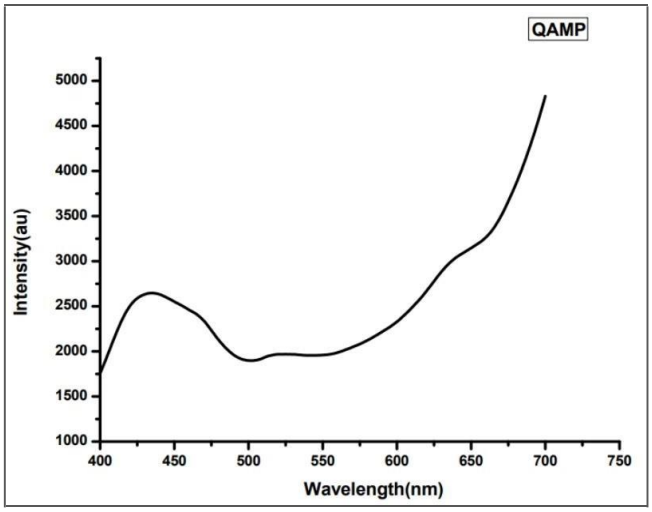

Figure 3.19: Fluorescence spectrum of QAMP

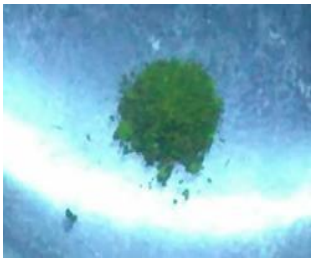

Figure 3.20: Solid-state fluorescence of QAMP

Figure 3.21: Liquid fluorescence of QAMP in methanol, acetone, hexane, ethyl alcohol and DMF

3.4 ANALYSIS OF QSAM (Quercetin+sulfanilamide)

3.4.1 Elemental Analysis

Elemental analysis of QSAM was conducted to examine the elemental composition of the Schiff base. QSAM has an empirical formula $C_{21}H_{16}O_8N_2S$. The results obtained are consistent with the proposed chemical formula of the assigned structure (*Table 4)*.

Compound	Empirical Formula	Formula Weight	Colour	Found (Calculated %)		
				C	H	N
QSAM	$C_{21}H_{16}O_8N_2S$	456.434	Green	56.06 (55.89)	4.36 (4.87)	5.31 (5.90)

Table 4: Elemental analysis of QSAM

3.4.2 UV-Visible Spectroscopy

The chemical structure and optical characteristics of the sample QSAM were investigated using Ultraviolet-visible spectroscopy. The UV-visible spectrum of QSAM was obtained in methanol (*Figure 3.22*). In the UV-visible spectrum, the primary transitions are $\pi \rightarrow \pi^*$ for aromatic rings around 180-350 nm and $n \rightarrow \pi^*$ for azomethine groups (C=N) around 300-450 nm. The sample QSAM exhibit peaks at 268 nm for transition within aromatic rings and 369 nm for transition within C=N group.

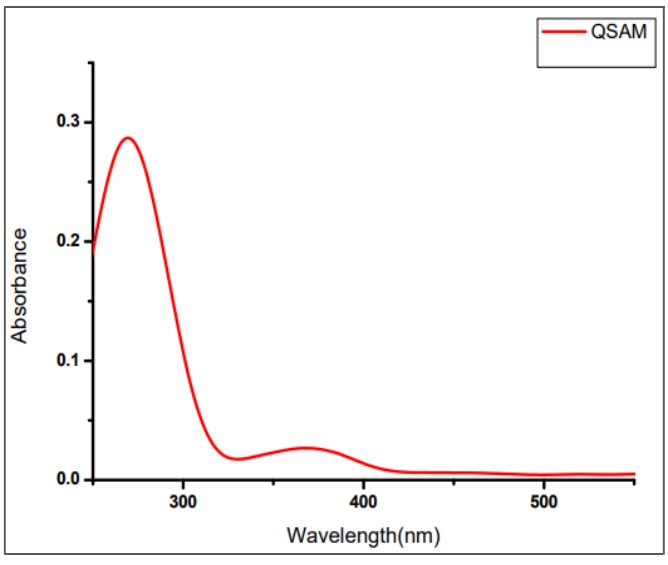

Figure 3.22: UV-visible spectrum of QSAM

3.4.3 Infrared Spectroscopy

The functional groups present and molecular structure of the sample QSAM were obtained from IR spectrum (*Figure 3.23*). A sharp peak at 1653.85 cm^{-1} was obtained for QSAM corresponding to the IR absorption peak of imine group (C=N) in the range 1690-1640 cm^{-1}. A peak at 3420.19 cm^{-1} was obtained corresponding to the absorption peak of phenolic (OH) group in the range 3500-3200 cm^{-1}.

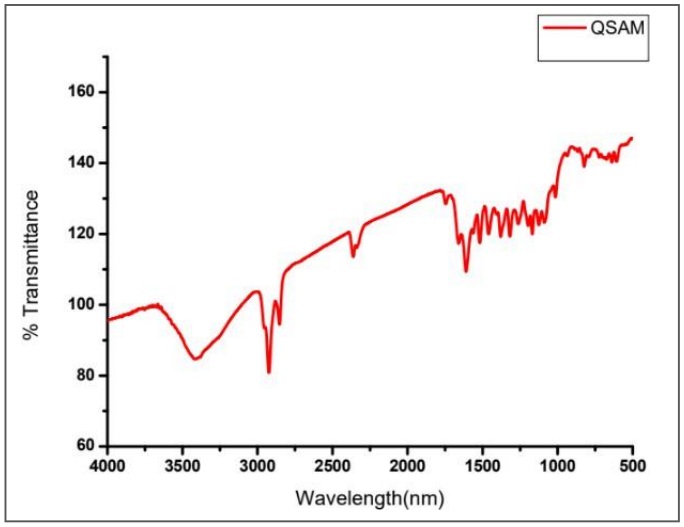

Figure 3.23: IR spectrum of QSAM

3.4.4 Nuclear Magnetic Resonance Spectroscopy

3.4.4.1 ^{1}H NMR Spectroscopy

^{1}H NMR spectrum of QSAM (*Figure 3.24*) provides the information about the number of hydrogen atoms and their relationships.

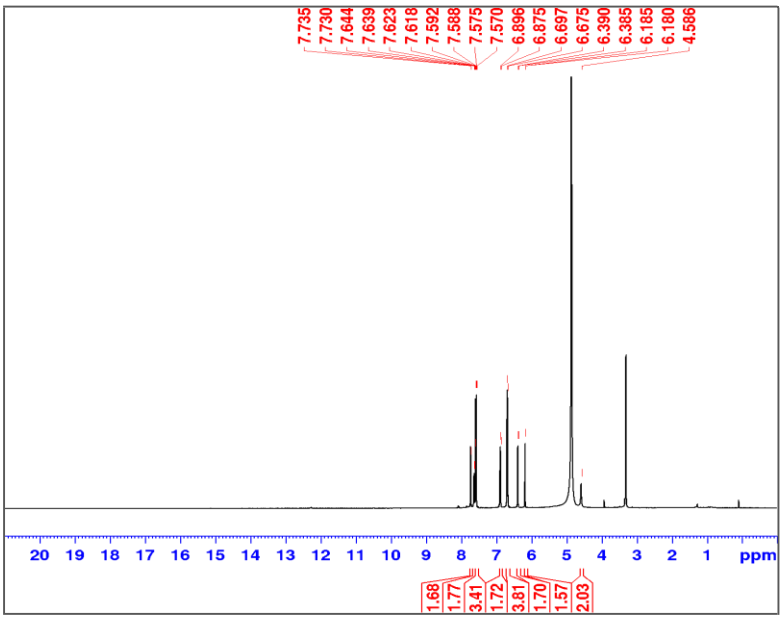

Figure 3.24: ^{1}H NMR spectrum of QSAM

^{1}H NMR (CH_3OH δ ppm): 4.58(2H, N-H), 6.1(2H, Ar-H), 6.3(1H, Ar-H), 6.6(2H, Ar-H), 6.8 (2H, Ar-H), 7.5 (2H, Ar-H), 7.6(2H, Ar-OH), 7.7(2H, OH), 7.8(1H, OH).

3.4.4.2 ^{13}C NMR Spectroscopy

^{13}C NMR spectrum of the sample QSAM (*Figure 3.25)* reveal the carbon skeleton of the compound.

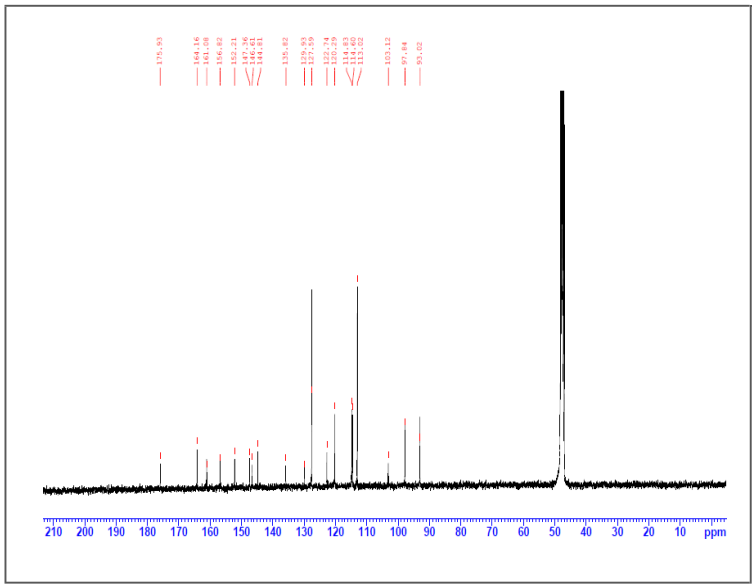

Figure 3.25: ^{13}C NMR spectrum of QSAM

^{13}C NMR (CH_3OH δ ppm): 93.02 (Ar-C), 97.84 (Ar-C), 103.12 (Ar-C), 113.02, 114.60 (Ar-C), 120.29(Ar-C), 122.74 (Ar-C), 129.39 (Ar-OH), 135.82(Ar-OH), 144.81(Ar-OH), 146.61 (AR-C-OH), 152.21 (Ar-CO), 161.08 (Ar-C-OH), 175.53(ArC=N).

3.4.5 Fluorescence Spectroscopy

The photoluminescence properties of the sample QSAM was obtained from the fluorescence spectrum (*Figure 3.26*). QSAM was excited at 350 nm and an emission wavelength was obtained at 426 nm. The solid-state and liquid-state fluorescence were observed under UV light (*Figure 3.27, 3.28*). The liquid-state fluorescence was examined in methanol, acetone, hexane, ethyl alcohol and DMF.

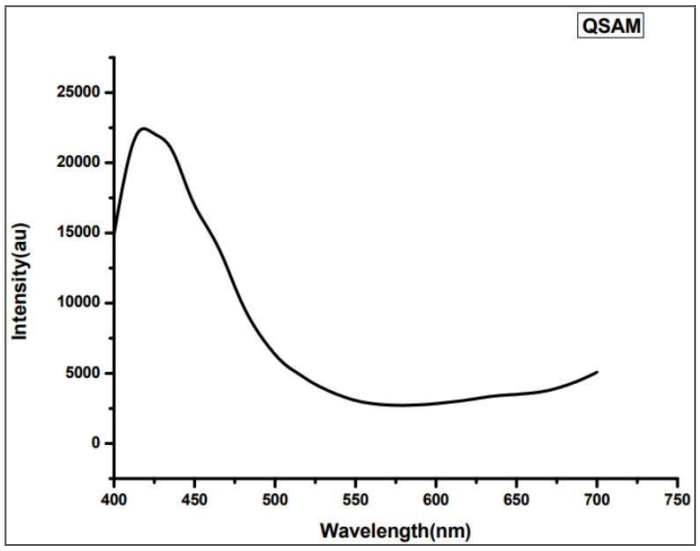

Figure 3.26: Fluorescence spectrum of QSAM

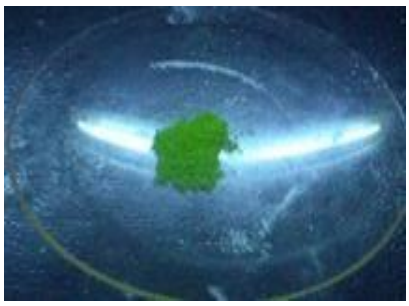

Figure 3.27: Solid-state fluorescence of QSAM

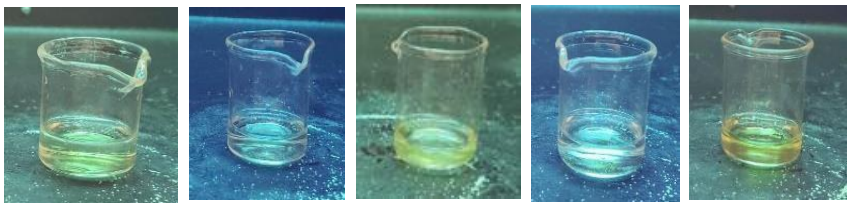

Pale yellow Yellow-orange

Figure 3.28: Liquid fluorescence of QSAM in methanol, acetone, hexane, ethyl alcohol and DMF

3.5 ANTI-INFLAMMATORY STUDY

Anti-inflammatory study was done using HRBC stabilization method. The prepared HRBC membrane stabilization assays of the four sample are given (Figure *3.29,3.30,3.31,3.*32). The HRBC membrane stabilization assay was used to analyze the anti-inflammatory properties of the samples QAAP, QSAM, QABD, and QAMP. Each sample showed remarkable membrane protective effects which were concentration dependent. Maximum protection percentages were noted at the highest tested concentration of 10mg/mL with QAMP achieving 73.805% protection and QABD and QSAM following . The standard provided the highest protection at 80.21% which was achieved with Diclofenac sodium. Based on these results, it can be stated that the examined samples have potential anti-inflammatory activity. The percentage inhibition of the 4 different Schiff bases is calculated. The values are tabulated in the below given tables (*Table 5,6,7,8*). From the percentage inhibition of samples at different concentration, four graph showing the anti-inflammation property of QAAP, QABD, QAMP, and QSAM were plotted (*Figure 3.33,3.34,3.35,3.36*).

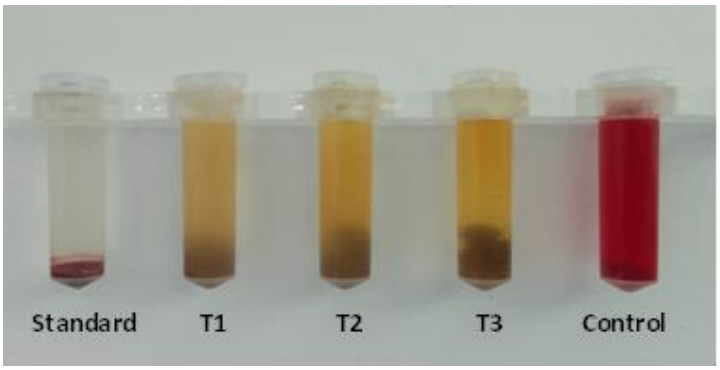

Figure 3.29: HRBC membrane stabilization assay of QAAP

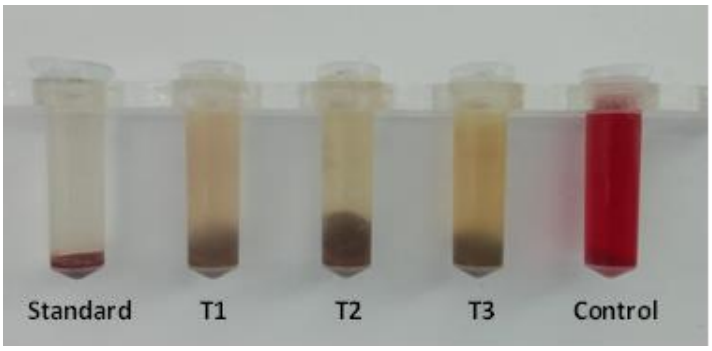

Figure 3.30: HRBC membrane stabilization assay of QABD

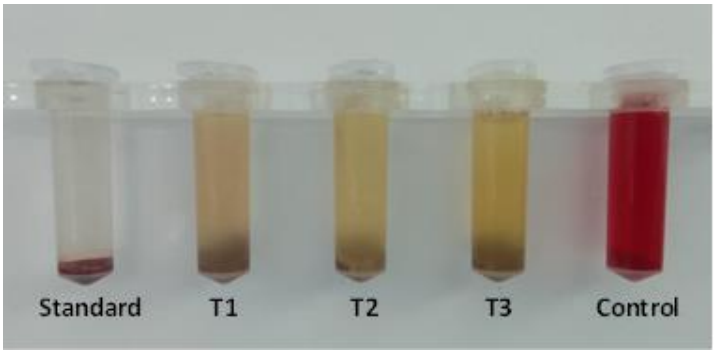

Figure 3.31: HRBC membrane stabilization assay of QAMP

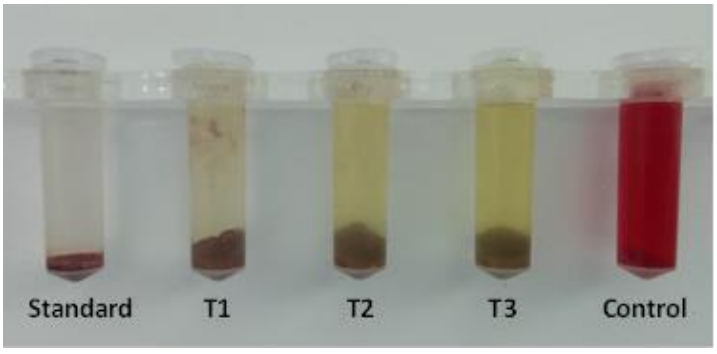

Figure 3.32: HRBC membrane stabilization assay of QSAM

Compound	Concentration of Sample (mg/ml)	% of Inhibition
QAAP	0.5	48.07
	2.5	55.09
	5	59.25
	10	60.91
	12.5	62.08

Table 5: Anti-Inflammatory activity of QAAP

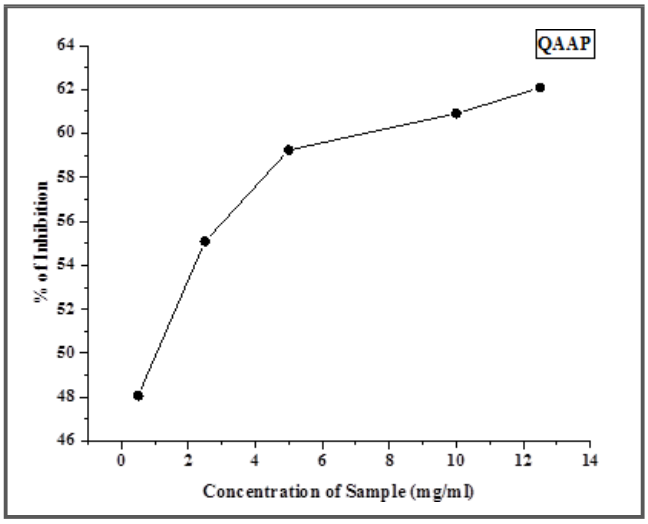

Figure 3.33: Anti-Inflammatory of QAAP

Compound	Concentration of Sample (mg/ml)	% of Inhibition
QABD	0.5	49.56
	2.5	70.48
	5	71.73
	10	73.39
	12.5	74.45

Table 6: Anti-Inflammatory activity of QABD

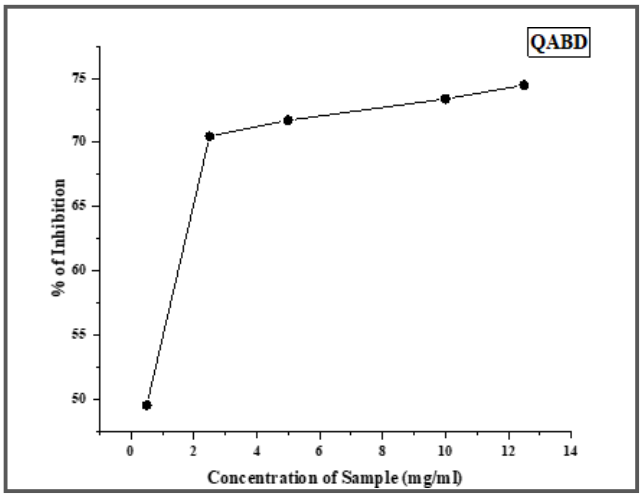

Figure 3.34: Anti-Inflammatory of QABD

Compound	Concentration of Sample (mg/ml)	% of Inhibition
QAMP	0.5	49.68
	2.5	69.23
	5	71.31
	10	73.8
	12.5	74.52

Table 7: Anti-Inflammatory activity of QAMP

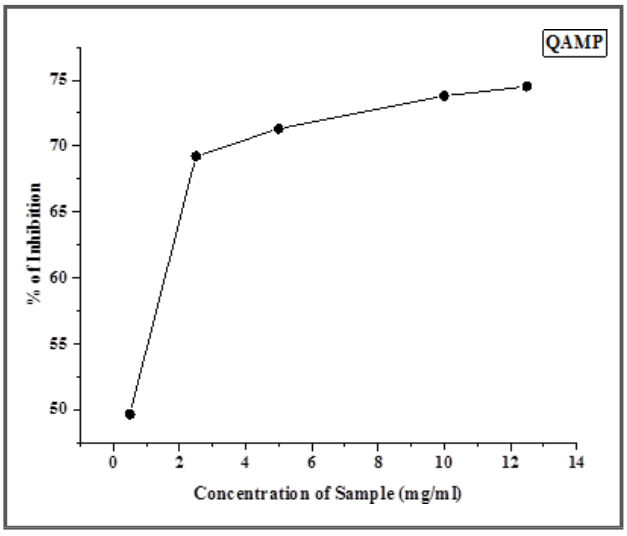

Figure 3.35: Anti-Inflammatory of QAMP

Compound	Concentration of Sample (mg/ml)	% of Inhibition
QSAM	0.5	52.75
	2.5	68.81
	5	72.97
	10	74.22
	12.5	76.34

Table 8: Anti-Inflammatory activity of QSAM

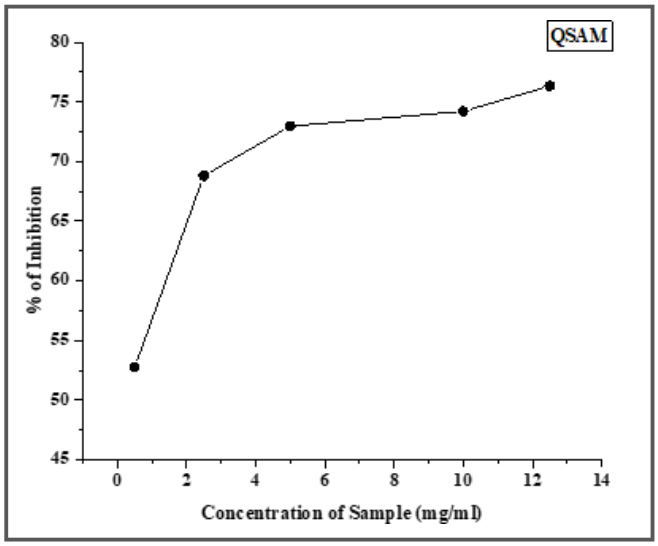

Figure 3.36: Anti-Inflammatory of QSAM

3.5.1 IC_{50} Value

IC_{50} (half-maximal inhibitory concentration) is a key parameter used in biochemistry to evaluate the potency of a compound in inhibiting a biological or biochemical function. It represents the concentration of a substance required to inhibit 50% of a specific target activity, such as an enzyme, receptor, or cellular response. IC_{50} value of each synthesized Schiff bases were obtained by plotting a graph between concentrations of

samples versus percentage of inhibition. IC_{50} value explains the concentration at which substance exhibits half of its maximum inhibition. IC_{50} value indicates the compound's ability to reduce inflammation by inhibiting key inflammatory mediators or enzymes. A lower IC_{50} value indicates a more potent inhibitor, meaning less compounds are needed to achieve a 50% inhibitory effect. IC_{50} value of QAAP, QABD, QAMP, QSAM are given in the table below (*Table 9*).

COMPOUND	**IC_{50} VALUES [mg/ml]**
QAAP	1.0854
QABD	0.5617
QAMP	0.5354
QSAM	0.5851
Ibuprofen	76.3273

Table 9: IC_{50} values

These IC_{50} values of synthesized Schiff bases were compared with ibuprofen a widely used non-steroidal anti-inflammatory drug and the IC_{50} values of the Schiff bases are much lower when compared to ibuprofen indicating these have higher inhibiting strength. Concluding that these could be developed as potent anti-inflammatory agents.

Chapter 4

Conclusions

In this study, four new Quercetin Schiff bases were synthesized, characterized and its anti-inflammatory activity were analyzed. These Schiff bases were synthesized by reflux condensation of sulfanilamide (QSAM), 3-aminobenzoic acid (QABD), 4-aminoantipyrene (QAAP) and 2-amino-5-methyl pyridine (QAMP) with Quercetin. These Quercetin Schiff bases were analyzed through various spectroscopic techniques such as FTIR, Elemental analysis, UV-visible, Fluorescence, ^{1}H and ^{13}C NMR. Through this analysis, a verified and satisfactory result for the formation of Quercetin Schiff bases was obtained. Furthermore, the anti-inflammatory potential of these synthesized quercetin Schiff bases was also assessed using HRBC membrane method and discussed in this study. From the anti-inflammatory studies, the IC_{50} values were obtained. The IC_{50} value of QSAM, QABD, QAAP and QAMP are 0.5851(mg/ml), 0.5617(mg/ml), 1.0854(mg/ml) and 0.5354(mg/ml) respectively. A relative study of the Schiff bases with ibuprofen was conducted from which QSAM, QABD, QAAP, QAMP were found to be more effective than ibuprofen.

References

1. Formica, J. V & Regelsont, W. *Review of the Biology of Quercetin and Related Bioflavonoids*. *Fd Chem. Toxic* vol. 33 (1995).
2. Shrivastava, N., Singh Baghel, S., Singh Baghel, R., Agrawal, P. & Rajput, S. *A Review of Quercetin: Antioxidant and Anticancer Properties*. www.wjpps.com (2012).
3. Mariani, C. *et al.* Flavonoid characterization and in vitro antioxidant activity of Aconitum anthora L. (Ranunculaceae). *Phytochemistry* **69**, 1220–1226 (2008).
4. Begum, A. N. & Terao, J. Protective effect of quercetin against cigarette tar extract-induced impairment of erythrocyte deformability. *J Nutr Biochem* **13**, 265–272 (2002).
5. Yarahmadi, A., Sarabi, M. M., Sayahi, A. & Zal, F. Protective effects of quercetin against hyperglycemia-induced oxidative stress in hepatic HepG2 cell line. *Avicenna J Phytomed* **11**, 269–280 (2021).
6. Xie, Y., Yang, W., Tang, F., Chen, X. & Ren, L. Antibacterial Activities of Flavonoids: Structure-Activity Relationship and Mechanism. *Curr Med Chem* **22**, 132–149 (2014).
7. Wang, S. *et al.* Bacteriostatic Effect of Quercetin as an Antibiotic Alternative In Vivo and Its Antibacterial Mechanism In Vitro. *J Food Prot* **81**, 68–78 (2018).
8. Yi Shu. Antibacterial activity of quercetin on oral infectious pathogens. *Afr J Microbiol Res* **5**, (2011).
9. Cruz-Correa, M. *et al.* Combination treatment with curcumin and quercetin of adenomas in familial adenomatous polyposis. *Clin Gastroenterol Hepatol* **4**, 1035–1038 (2006).

10. Zhou, H. *et al.* Co-delivery of doxorubicin and quercetin by Janus hollow silica nanomotors for overcoming multidrug resistance in breast MCF-7/Adr cells. *Colloids Surf A Physicochem Eng Asp* **658**, 130654 (2023).
11. Salehi, B. *et al.* Therapeutic Potential of Quercetin: New Insights and Perspectives for Human Health. *ACS Omega* **5**, 11849 (2020).
12. Guan, F., Wang, Q., Bao, Y. & Chao, Y. Anti-rheumatic effect of quercetin and recent developments in nano formulation. *RSC Adv* **11**, 7280–7293 (2021).
13. Chaudhary, S., Sharma, S., Fuloria, S. & Sharma, P. K. Anti-Inflammatory and Anti-Arthritis Activity of Quercetin: A Comprehensive Review. *Curr Rheumatol Rev* **20**, 1–16 (2024).
14. Chekalina, N. *et al.* Quercetin reduces the transcriptional activity of NF-kB in stable coronary artery disease. *Indian Heart J* **70**, 593 (2018).
15. Chen, L. *et al.* Inflammatory responses and inflammation-associated diseases in organs. *Oncotarget* **9**, 7204–7218 (2017).
16. Ferrero-Miliani, L., Nielsen, O. H., Andersen, P. S. & Girardin, S. E. Chronic inflammation: importance of NOD2 and NALP3 in interleukin-1beta generation. *Clin Exp Immunol* **147**, 227–235 (2007).
17. Kumar, R., Clermont, G., Vodovotz, Y. & Chow, C. C. The dynamics of acute inflammation. *J Theor Biol* **230**, 145–155 (2004).
18. Pahwa, R., Goyal, A. & Jialal, I. Chronic Inflammation. *Pathobiology of Human Disease: A Dynamic Encyclopedia of Disease Mechanisms* 300–314 (2023) doi:10.1016/B978-0-12-386456-7.01808-6.
19. Volluri, S. S., Bammidi, S. R., Chippada, S. C. & Vangalapati, M. In vitro anti-inflammatory activity of methanolic extract of bacopa monniera by HRBC membrane stabilisation. *Biosci Biotechnol Res Asia* **8**, 333–336 (2011).

20. Balamurugan, V., Sridhivya, M., Dharani, R., Selvakumar, S. & Vasanth, K. Phytochemical Screening, Antioxidant, Antidiabetic and Anticancer Activities of Elaeocarpus variabilis Fruit. *Turkish Journal of Agriculture - Food Science and Technology* **10**, 1352–1362 (2022).